

**Electronic structure trends in the  $\text{Sr}_{n+1}\text{Ru}_n\text{O}_{3n+1}$  family ( $n = 1, 2, 3$ )**M. Malvestuto,<sup>1</sup> E. Carleschi,<sup>2,3,\*</sup> R. Fittipaldi,<sup>4,5</sup> E. Gorelov,<sup>6</sup> E. Pavarini,<sup>6,†</sup> M. Cuoco,<sup>4,5,‡</sup> Y. Maeno,<sup>7</sup>  
F. Parmigiani,<sup>2,3</sup> and A. Vecchione<sup>4,5</sup><sup>1</sup>*Sincrotrone Trieste, Area Science Park, I-34012 Basovizza, Trieste, Italy*<sup>2</sup>*CNR-IOM, TASC Laboratory, Area Science Park, I-34012 Basovizza, Trieste, Italy*<sup>3</sup>*Dipartimento di Fisica, Università degli Studi di Trieste, I-34127 Trieste, Italy*<sup>4</sup>*CNR-SPIN, I-84084 Fisciano, Salerno, Italy*<sup>5</sup>*Dipartimento di Fisica "E.R. Caianiello," Università di Salerno, I-84084 Fisciano, Salerno, Italy*<sup>6</sup>*Institut für Festkörperforschung and Institute for Advanced Simulation, Forschungszentrum Jülich, D-52425 Jülich, Germany*<sup>7</sup>*Department of Physics, Kyoto University, Kyoto 606-8502, Japan*

(Received 27 January 2011; published 19 April 2011)

The identification of electronic states and the analysis of their evolution with  $n$  is key to understanding  $n$ -layered ruthenates. To this end, we combine polarization-dependent O  $1s$  x-ray absorption spectroscopy, high-purity  $\text{Sr}_{n+1}\text{Ru}_n\text{O}_{3n+1}$  ( $n = 1, 2, 3$ ) single crystals, and *ab initio* and many-body calculations. We find that the energy splitting between the empty  $x^2 - y^2$  and  $3z^2 - 1$  state is considerably smaller than previously suggested and that, remarkably, Sr bands are essential to understanding the spectra. At low energy, we identify the main difference among the materials with a substantial rearrangement of  $t_{2g}$  orbital occupations with increasing  $n$ . This rearrangement is controlled by the interplay of Coulomb repulsion, dimensionality, and changes in the  $t_{2g}$  crystal field.

DOI: [10.1103/PhysRevB.83.165121](https://doi.org/10.1103/PhysRevB.83.165121)

PACS number(s): 71.20.Be, 71.15.-m, 71.27.+a, 78.70.Dm

**I. INTRODUCTION**

The ruthenates of the Ruddlesden-Popper family  $A_{n+1}\text{Ru}_n\text{O}_{3n+1}$  ( $A = \text{Ca}$  and  $\text{Sr}$ ) (Fig. 1) are unique among transition-metal oxides because the change in the number  $n$  of  $\text{RuO}_2$  layers leads to a variety of collective phenomena: spin-triplet chiral superconductivity<sup>3</sup> and Fermi-surface anomalies<sup>4</sup> ( $n = 1$ ); heavy  $d$ -electron masses<sup>5–8</sup> ( $n = 1, 2$ ); colossal magnetoresistance,<sup>9</sup> proximity to a metamagnetic quantum critical point, and nematic fluid behavior<sup>10–12</sup> ( $n = 2$ ); and itinerant ferromagnetism and metamagnetism ( $n = 3$ ).<sup>13–15</sup> It is believed that such diversity stems from the interplay of orbital, spin, and lattice degrees of freedom in the partially filled Ru  $4d$  shells ( $t_{2g}^4 e_g^0$ ). Understanding how the change in  $n$ , which reflects the dimensionality, modifies this interplay is thus crucial to explaining the physics of these ruthenates.

Single-layered ( $n = 1$ ) systems are regarded as quasi-two-dimensional. The  $\frac{2}{3}$ -filled  $t_{2g}$  bands split into a wide  $xy$  and two narrow  $xz$  and  $yz$  bands, with bandwidth ratio  $R = W_{xz/yz}/W_{xy} \sim 0.5$  and occupations  $n_{xy}$ ,  $n_{xz}$ , and  $n_{yz}$ . Many-body studies of three-band Hubbard models have shown that a small  $R$ , a crystal-field splitting  $\Delta$ , and a finite Coulomb exchange interaction can have a large impact on the electronic structure, leading in some cases to negative<sup>16</sup> orbital polarization  $p = n_{xy} - (n_{xz} + n_{yz})/2$  and even to orbital-selective Mott transitions.<sup>17,18</sup> Infinite-layered ( $n \rightarrow \infty$ ) systems are three dimensional. By increasing  $n$ , the effective dimensionality increases;  $W_{xz/yz}$  approaches the  $xy$ -band width ( $R \sim 1$ ), while, due to the change in both structure and lattice distortions, the crystal-field and the hopping integrals can be strongly modified; different parameter regimes can be reached. Furthermore, for real materials, there are indications that  $e_g$  states may also affect material properties.<sup>6,19,20</sup> The key parameters to determine are thus the crystal-field splittings in the Ru  $4d$  shell, as well as the orbital occupations.

In this work we focus on the  $\text{Sr}_{n+1}\text{Ru}_n\text{O}_{3n+1}$  series. The recent availability of high-quality  $\text{Sr}_4\text{Ru}_3\text{O}_{10}$  single crystals, combined with comparably pure  $\text{Sr}_3\text{Ru}_2\text{O}_7$  and  $\text{Sr}_2\text{RuO}_4$  ones, allows us to reveal, for the first time, the evolution of the unoccupied electronic structure in the family. We use polarization-dependent O  $1s$  x-ray-absorption spectroscopy (XAS) and analyze the spectra by means of *ab initio* and many-body methods. We find that, contrary to previous suggestions,<sup>20,21</sup> the splitting between  $e_g$  states is less than 1 eV, while, surprisingly, Sr bands are essential to understanding the spectra. We show that, at low energy, the main difference among the materials is a substantial rearrangement of  $t_{2g}$  orbital occupations. This rearrangement is controlled by the interplay of dimensionality, the  $t_{2g}$  crystal field, and Coulomb repulsion.

**II. METHOD**

High-quality  $\text{Sr}_{1+n}\text{Ru}_n\text{O}_{3n+1}$  ( $n = 1, 2, 3$ ) single crystals have been grown by the flux-feeding floating-zone technique, with Ru self-flux,<sup>22</sup> while exploiting recent advances in fabrication techniques.<sup>22–24</sup> The structure and crystalline qualities of the samples were assessed by a high-resolution x-ray diffractometer (Philips, model X' Pert MRD), with a Cu  $K\alpha$  source. The x-ray-diffraction pattern taken on cleaved surface of  $\text{Sr}_2\text{RuO}_4$ ,  $\text{Sr}_3\text{Ru}_2\text{O}_7$ , and  $\text{Sr}_4\text{Ru}_3\text{O}_{10}$  crystals, shown in Fig. 2, confirm the absence of spurious phases. All the diffraction peaks can be identified with the expected ( $00l$ ) Bragg reflections of the Sr-based Ruddlesden-Popper ruthenates structures. Absorption spectra at the O  $K$  edge were measured at the Beamline for Advanced Dichroism (BACH) at Elettra,<sup>25</sup> in the total-electron-yield mode<sup>26</sup> and at  $T = 115$  K. All sample surfaces were prepared *in situ* by cleaving in a high ultravacuum. The O  $1s$  XAS spectra for the three systems were acquired with fixed photon polarization and an incident angle  $\theta_{\text{inc}}$  varying from  $0^\circ$  to  $70^\circ$ . The XAS data were normalized to the beam intensity at 560 eV, which is well above

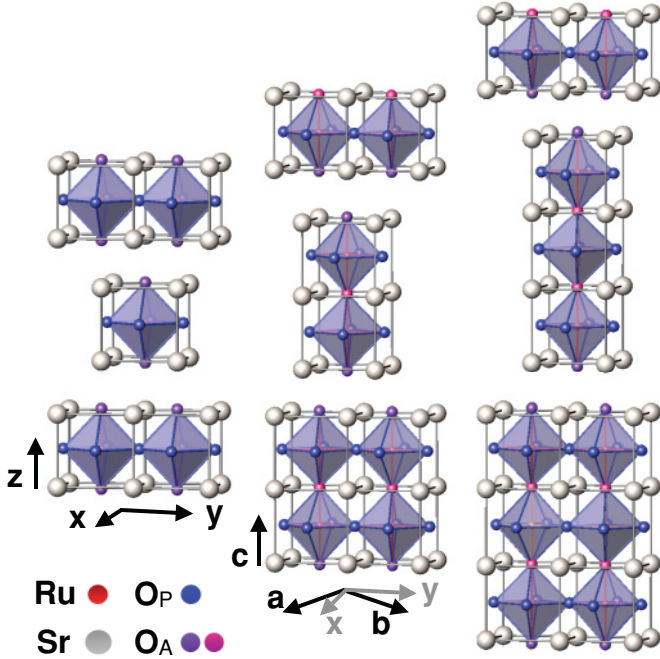


FIG. 1. (Color online) Left to right: Crystal structure of  $\text{Sr}_2\text{RuO}_4$ ,  $\text{Sr}_3\text{Ru}_2\text{O}_7$ , and  $\text{Sr}_4\text{Ru}_3\text{O}_{10}$ .<sup>1</sup> The tetragonal ( $\text{Sr}_2\text{RuO}_4$ ) and pseudotetragonal<sup>2</sup> ( $\text{Sr}_3\text{Ru}_2\text{O}_7$  and  $\text{Sr}_4\text{Ru}_3\text{O}_{10}$ ) axes are indicated by  $x$ ,  $y$ , and  $z$ .

the absorption threshold  $E_0 \sim 528$  eV. The incoming-photon electric field  $\vec{E}$  has an in-plane component  $E_{xy} = |\vec{E}| \cos \theta_{\text{inc}}$  and an out-of-plane component  $E_z = |\vec{E}| \sin \theta_{\text{inc}}$ , parallel to the  $c$  axis. Due to the dipole selection rules, the in-plane field induces  $\text{O } 1s \rightarrow \text{O } 2p_{x/y}$  excitations only, while the out-of-plane field induces exclusively  $\text{O } 1s \rightarrow \text{O } 2p_z$  transitions. Thus, by changing  $\theta_{\text{inc}}$ , empty states with different symmetries are probed.

In order to identify the electronic states we first compare the experiments with *ab initio* calculations based on the local-density approximation (LDA). For  $\text{Sr}_2\text{RuO}_4$  and  $\text{Sr}_3\text{Ru}_2\text{O}_7$  we compare our LDA bands with published band structures<sup>19,27</sup> and find good agreement. In the next step we use the down-folding technique based on the  $N$ th-order muffin-tin orbital method to construct material-specific Wannier functions that span the Ru  $4d$  bands; we then obtain hopping integrals and crystal-field splittings.<sup>28</sup> Finally, for relevant cases, from these Wannier functions we build material-dependent  $t_{2g}$  Hubbard models and solve them using the dynamical mean-field theory (DMFT), within the LDA+DMFT approach.<sup>29</sup> We adopt the LDA+DMFT implementation discussed in Ref. 2, which is based on a weak-coupling continuous-time quantum Monte Carlo solver.<sup>30</sup>

### III. RESULTS

The XAS spectra for horizontal polarization are shown in Fig. 3. There are two main absorption regions: a low-energy one that extends from  $E_0$  to  $E_1 = 530$  eV and a high-energy one from  $E_1$  to  $E_2 = 536$  eV. In the low-energy region,  $\text{Sr}_2\text{RuO}_4$  exhibits a double-peak structure ( $A$  and  $B$  features), which can be ascribed<sup>31</sup> to the energy difference between

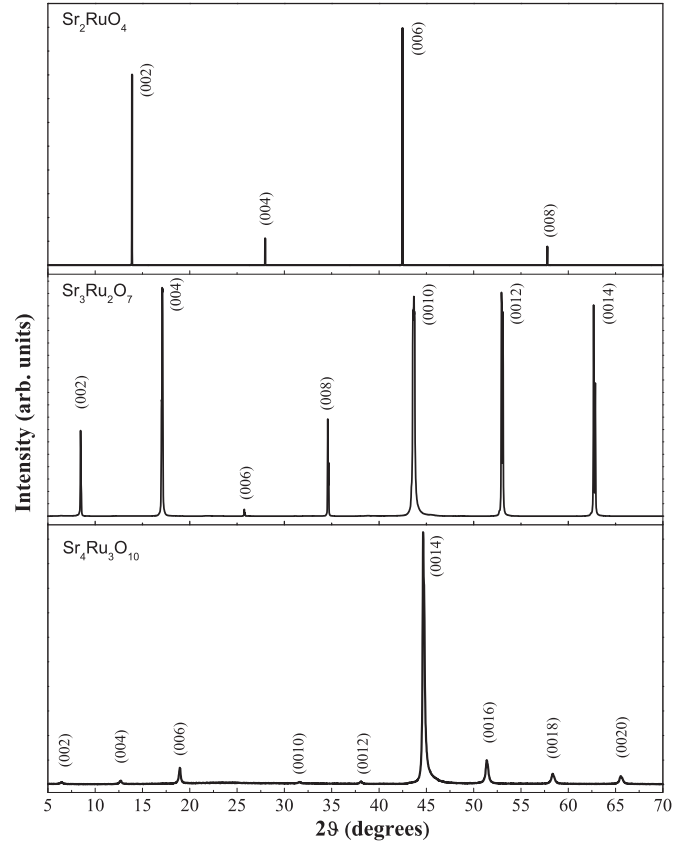


FIG. 2. X-ray-diffraction patterns of a cleaved (001) surface of  $\text{Sr}_2\text{RuO}_4$ ,  $\text{Sr}_3\text{Ru}_2\text{O}_7$ , and  $\text{Sr}_4\text{Ru}_3\text{O}_{10}$  crystals, grown with the flux-growth floating-zone method. The spectra show the absence of any spurious phase and all the peaks are indexed as  $(00l)$  peaks of the Sr-based Ruddelsden-Popper ruthenates structures.

apical ( $\text{O}_A$ ) and planar ( $\text{O}_P$ ) oxygen  $1s$  core levels. The double peak turns into a single peak with a shoulder in  $\text{Sr}_3\text{Ru}_2\text{O}_7$  and  $\text{Sr}_4\text{Ru}_3\text{O}_{10}$ . The energy separation between peaks  $B$  and  $C$  is about 4 eV in  $\text{Sr}_2\text{RuO}_4$  and slightly increases to  $n = 2, 3$ , mainly because the feature  $C$  drifts to higher energy. The spectral weight between  $B$  and  $C$  increases as  $n$  grows. In all systems, a progressive spectral weight transfer from the high- to the low-energy region is observed by increasing  $\theta_{\text{inc}}$  from  $0^\circ$  to  $70^\circ$ . Finally, for  $0^\circ$ , peak  $C$  is considerably reduced for the bilayered and trilayered materials.

For horizontal polarization, the XAS intensity can be estimated<sup>32</sup> as  $I(\theta_{\text{inc}}, \omega) = \frac{1}{2}[\rho_x(\omega) + \rho_y(\omega)] \cos^2 \theta_{\text{inc}} + \rho_z(\omega) \sin^2 \theta_{\text{inc}}$ . The factors  $\rho_\alpha(\omega) = \sum_i \rho_{\alpha i}(\omega - \epsilon_i^{1s})$ , with  $\alpha = x, y, z$ , are sums of the orbital-resolved O density of empty states  $\rho_{\alpha i}(\omega - \epsilon_i^{1s})$ , while  $-\epsilon_i^{1s}$  is the  $1s$  core energy (with respect to the Fermi level) of oxygen  $i$ . In Fig. 4 we compare XAS experiments with  $I(\theta_{\text{inc}}, \omega)$  obtained from LDA calculations. The agreement with experiments is good in the full energy window. A crucial ingredient is the spread in O  $1s$  core energies. In the case of  $\text{Sr}_2\text{RuO}_4$  this amounts to a negative shift of  $\sim 1.3$  eV of the planar ( $\text{O}_P$ ) oxygen  $1s$  level with respect to the apical ( $\text{O}_A$ ) oxygen  $1s$  level. For  $\text{Sr}_3\text{Ru}_2\text{O}_7$  there are one planar and two nonequivalent apical oxygens ( $\text{O}_{A1}$  and  $\text{O}_{A2}$ ); the core energy shifts are  $\sim 0.8$  eV ( $\text{O}_{A2}$ ) and  $\sim 1.2$  eV ( $\text{O}_P$ ). Finally, for  $\text{Sr}_4\text{Ru}_3\text{O}_{10}$  the apical oxygen

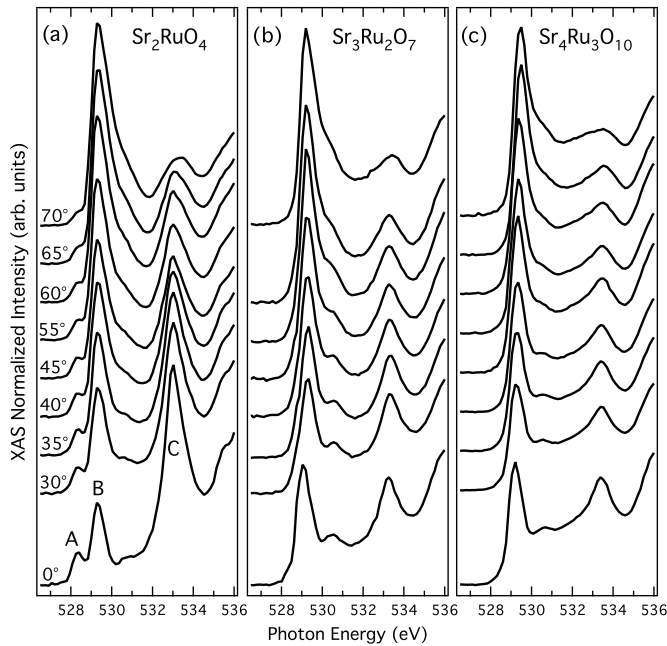


FIG. 3. XAS spectra ( $T = 115$  K) at the O  $K$  edge for (a)  $\text{Sr}_2\text{RuO}_4$ , (b)  $\text{Sr}_3\text{Ru}_2\text{O}_7$ , and (c)  $\text{Sr}_4\text{Ru}_3\text{O}_{10}$ . The spectra are shown for several values of  $\theta_{\text{inc}}$ , the angle between  $\mathbf{c}$  and the incoming x rays. The cleaved surface is perpendicular to the  $\mathbf{c}$  axis (Fig. 1). A, B, and C label the most relevant features.

core-energy shifts are  $\sim 0$ – $0.4$  eV while the planar ones are  $\sim 0.7$ – $1.1$  eV.<sup>33</sup>

Given the good agreement between LDA results and experiments, we proceed to the identification of the electronic states. We start with the analysis of the low-energy-absorption region. Figure 4 shows that at the absorption threshold (feature A in  $\text{Sr}_2\text{RuO}_4$ ) the main contribution comes from  $\text{O}_A$ , while peak B is mainly due to  $\text{O}_P$ . We find that in this energy window O  $p$  electrons hybridize mostly with Ru  $t_{2g}$  electrons.

In the case of  $\text{Sr}_2\text{RuO}_4$   $W_{xy}$  is considerably larger than  $W_{xz/yz}$ ; the ratio  $R \sim 0.5$ . The highest-energy crystal-field Wannier orbital is  $|xy\rangle$ ; the  $|xz\rangle$  and  $|yz\rangle$  Wannier states are degenerate and  $\Delta \equiv E_{xz/yz} - E_{xy} \sim -60$  meV. The orbital polarization  $p_{\text{LDA}} \sim -0.35$ . The  $xz$  and  $yz$  orbitals mostly hybridize with  $\text{O}_A$   $x$  and  $y$  and  $\text{O}_P$   $z$ , while  $xy$  orbitals hybridize with  $\text{O}_P$   $x$  and  $y$ . Thus, for  $\theta_{\text{inc}} = 0^\circ$ , feature A mainly originates from the  $xz$  and  $yz$  bands, while peak B comes from the  $xy$  band. With increasing  $\theta_{\text{inc}}$  the contribution of  $\rho_x + \rho_y$  decreases, while that from  $\rho_z$  increases. Thus peak A progressively decreases, while peak B changes its character from  $xy$  to  $xz/yz$ . This assignment is in agreement with previous works.<sup>20,21,31</sup> The ratio  $I(70^\circ, \omega)/I(0^\circ, \omega)$  is small for peak A because the contribution from  $\text{O}_A$   $z$  states is tiny; however, the ratio is  $\sim 2$ – $3$  for peak B because  $xy$  and  $xz + yz$  states couple to the same number of  $\text{O}_P$  states and  $R \sim 0.5$ .

In the case of  $\text{Sr}_3\text{Ru}_2\text{O}_7$  and  $\text{Sr}_4\text{Ru}_3\text{O}_{10}$ , due to the large spread in core-energy shifts, peak A splits and appears only as a shoulder of peak B, while, in the latter, the  $xz/yz$  and  $xy$  features partially overlap even for  $\theta_{\text{inc}} = 0^\circ$ . This leads to a line-shape modification of peak B and, for  $\text{Sr}_4\text{Ru}_3\text{O}_{10}$ , an energy shift of the maximum of  $\sim 0.4$  eV with increasing  $\theta_{\text{inc}}$  from  $0^\circ$  to  $70^\circ$  (Fig. 3).  $W_{xz/yz}$  rapidly increases and the

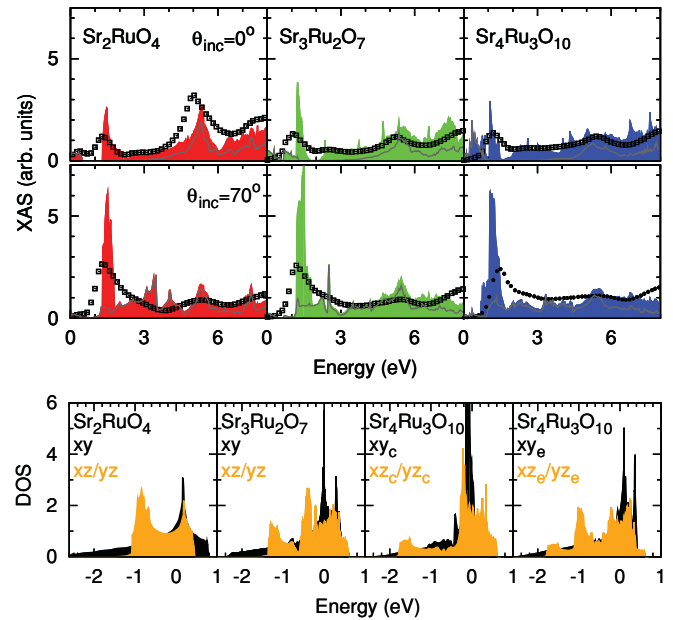


FIG. 4. (Color online) Top: XAS experimental data (open squares) and LDA results (filled curves) for  $\theta_{\text{inc}} = 0^\circ$  and  $70^\circ$ . The energy zero is the absorption threshold ( $E_0$ ); the normalization is the number of atoms per cell. The gray lines show the apical oxygen contribution. Bottom:  $t_{2g}$  density of states (states/eV) per Ru site. For  $\text{Sr}_4\text{Ru}_3\text{O}_{10}$  both central Ru (c) and external Ru (e) contributions are shown. Energy zero is denoted by  $\varepsilon_F$ .

bandwidth ratio approaches the infinite layers limit:  $R \sim 0.7$  in  $\text{Sr}_3\text{Ru}_2\text{O}_7$  and  $R \sim 0.8$  in  $\text{Sr}_4\text{Ru}_3\text{O}_{10}$ . The crystal-field orbitals are affected by the structural changes. Crucial aspects are changes not only in RuO bonds but also in SrRu and SrO distances and in the Sr cage. In the case of  $\text{Sr}_3\text{Ru}_2\text{O}_7$  we find that the lowest-energy orbital is  $|xy\rangle$  and  $\Delta \sim 45$  meV. The orbital polarization increases with respect to  $\text{Sr}_2\text{RuO}_4$ :  $p_{\text{LDA}} \sim -0.05$ . In  $\text{Sr}_4\text{Ru}_3\text{O}_{10}$  there is a distribution of small splittings, with  $\Delta \sim 120$  meV for the Ru in the central layers and  $\Delta \sim -90$  meV for the Ru in the external ones. Correspondingly, the total polarization  $p_{\text{LDA}} \sim 0$ , with  $p_{\text{LDA}} \sim 0.5$  for the central layer and  $p_{\text{LDA}} \sim -0.25$  for the external layers.

Our results show that at low energy the most significant difference among the three systems is the rearrangement of  $t_{2g}$  orbital occupations. We find that this rearrangement stems from the interplay between the dimensionality and the  $t_{2g}$  crystal field and it is associated with a change in the position of the Fermi level  $\varepsilon_F$  in the density of states (DOSs) (Fig. 4). At  $\frac{2}{3}$  filling, a small ratio  $R$  ( $n = 1$ ) favors the occupation of the  $xz$  and  $yz$  states ( $p < 0$ ), while a large positive  $\Delta$  favors the occupation of the  $xy$  states ( $p > 0$ ) (Ref. 2) and eventually pushes the  $xy$ -band van Hove singularity ( $\varepsilon_{\text{vHS}}^{xy}$ ) to the left of  $\varepsilon_F$ . For  $n \rightarrow \infty$ , in the absence of distortions,  $R \rightarrow 1$ ,  $p \rightarrow 0$ , and  $\varepsilon_F \rightarrow \varepsilon_{\text{vHS}}^{xy}$ ; the effects of the crystal field and distortions, however, become progressively stronger. In  $\text{Sr}_2\text{RuO}_4$ ,  $\Delta \sim -60$  meV; a positive  $\Delta \sim 60$  meV would yield a small  $p \sim 0.1$ ,  $\varepsilon_F \sim \varepsilon_{\text{vHS}}^{xy}$ , and  $\rho_{xz/yz}(\varepsilon_F)$  with positive curvature (favorable to metamagnetism<sup>34</sup>). For  $n = 2, 3$  we find that the calculated crystal field already yields a small or positive polarization and  $\varepsilon_F \sim \varepsilon_{\text{vHS}}^{xy}$ . Thus, while the actual position of  $\varepsilon_F$  depends on the details, ferromagnetic and

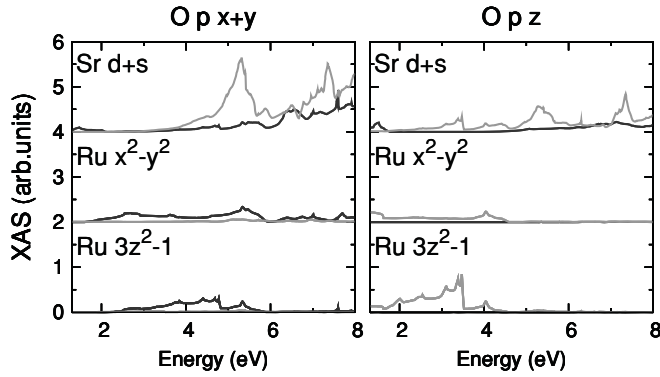


FIG. 5.  $\text{Sr}_2\text{RuO}_4$ : Sr  $d+s$  and Ru  $e_g$  contributions to the XAS intensity (Fig. 4). The dark gray curves show  $O_p$  XAS (with a 1.3-eV shift) and the light gray curves show  $O_A$  XAS.  $E_0 = 0$ . Left:  $O_x$  and  $y$ . Right:  $O_z$ .

metamagnetic instabilities appear to be more likely with an increasing number of layers  $n$ .

Electronic-correlation effects can modify orbital occupations.<sup>35</sup> To evaluate such effects we perform many-body LDA+DMFT calculations for the three-band Hubbard models constructed from the  $t_{2g}$  Wannier functions. We take as parameters  $U = 3.1$  eV and  $J = 0.7$  eV, in line with theoretical estimates.<sup>2,36</sup> We find that  $p$  is somewhat smaller than in the LDA: At 290 K,  $p_{\text{DMFT}} \sim -0.11$  for  $\text{Sr}_2\text{RuO}_4$  and  $p_{\text{DMFT}} \sim 0$  for  $\text{Sr}_3\text{Ru}_2\text{O}_7$ . Thus, due to many-body effects, holes are partially transferred from the  $xy$  bands to the  $xz$  and  $yz$  bands;<sup>16</sup> however, down to 290 K the trend remains the same as in the LDA.

Let us now analyze the high-energy-absorption region. For  $\text{Sr}_2\text{RuO}_4$ , the Ru and Sr contributions to the XAS are shown in Fig. 5. We find that  $e_g$  holes contribute right below 530 eV and extend to the full high-energy sector. The  $t_{2g}$ - $e_g$  crystal-field splitting is about 3.4–3.5 eV in all materials, in line with previous estimates,<sup>20</sup> while the splitting within  $e_g$  states<sup>37</sup> is 0.7 eV in  $\text{Sr}_2\text{RuO}_4$  and 0.3 eV or smaller in  $\text{Sr}_3\text{Ru}_2\text{O}_7$  and  $\text{Sr}_4\text{Ru}_3\text{O}_{10}$ , i.e., considerably less than the surprisingly large values ( $\sim 2$ – $3$  eV) previously inferred from XAS data.<sup>20,21</sup> In

$\text{Sr}_2\text{RuO}_4$ , Ru  $3z^2 - 1$  states contribute the most between 529 and 532 eV, through coupling to  $O_A z$ , and between 531 and 534 eV, through coupling to  $O_p x$  and  $y$  (Fig. 5). By increasing the number of  $\text{RuO}_2$  layers the  $3z^2 - 1$  band becomes broader, so that its contribution spreads to a larger-energy window. Ru  $x^2 - y^2$  bands contribute the most, for all three materials, between 530 and 535 eV, through coupling to  $O_p x$  and  $y$ . The coupling to apical  $O z$  states is small (but not zero) around 532 eV, in line with previous suggestions.<sup>20</sup>

Sr states also hybridize with  $O p$  orbitals. Remarkably, they start to be relevant at 531 eV, as Fig. 5 shows. In  $\text{Sr}_2\text{RuO}_4$ , Sr  $xz$  and  $yz$  strongly contribute to peak C, mainly through hybridization with  $x$  and  $y$  of the neighboring  $O_A$  along  $c$  (Fig. 5, top left); this leads to a revision of previous interpretations,<sup>20,21</sup> which ascribed peak C only to Ru  $x^2 - y^2$  states. When  $n$  increases the Sr contribution decreases, as only atoms in the external layers couple to apical  $x$  and  $y$ .

#### IV. CONCLUSION

In conclusion, by combining XAS with *ab initio* and many-body calculations, we understand basic aspects of the electronic structure of the  $\text{Sr}_{n+1}\text{Ru}_n\text{O}_{3n+1}$  series. We found that the splitting within  $e_g$  states is less than 1 eV, similarly to  $3d$  transition-metal oxides, and, surprisingly, Sr  $d$  bands are crucial to understanding the XAS spectra. These conclusions are likely to apply to all Sr and Ca layered  $4d$  perovskites of the Ruddlesden-Popper family. Finally, we have shown that, due to the interplay among dimensionality, the  $t_{2g}$  crystal field, and Coulomb repulsion, there is a substantial rearrangement of the  $t_{2g}$  orbital occupation in the series. This reflects a shift in the position of the van Hove singularities close to the Fermi level, which could explain<sup>19,34</sup> the increased tendency to ferromagnetism and metamagnetism for  $n = 2, 3$  and could be the root<sup>8,34</sup> of the diversity of behaviors in the family.

#### ACKNOWLEDGMENTS

E.G. and E.P. acknowledge the Jülich BlueGene/P Grant No. JIFF41, as well as financial support by the Deutsche Forschungsgemeinschaft through the research unit FOR 1346.

\*Present address: Department of Physics, University of Johannesburg, P.O. Box 524, Auckland Park 2006, South Africa.

†e.pavarini@fz-juelich.de

‡mario.cuoco@cnr.it

<sup>1</sup>H. Shaked, J. D. Jorgensen, O. Chmaissem, S. Ikeda, and Y. Maeno, *J. Solid State Chem.* **154**, 361 (2000); M. K. Crawford, R. L. Harlow, W. Marshall, Z. Li, G. Cao, R. L. Lindstrom, Q. Huang, and J. W. Lynn, *Phys. Rev. B* **65**, 214412 (2002).

<sup>2</sup>E. Gorelov, M. Karolak, T. O. Wehling, F. Lechermann, A. I. Lichtenstein, and E. Pavarini, *Phys. Rev. Lett.* **104**, 226401 (2010).

<sup>3</sup>Y. Maeno, H. Hashimoto, K. Yoshida, S. Nishizaki, T. Fujita, J. G. Bednorz, and F. Lichtenberg, *Nature (London)* **372**, 532 (1994); A. P. Mackenzie and Y. Maeno, *Rev. Mod. Phys.* **75**, 657 (2003).

<sup>4</sup>M. Neupane, P. Richard, Z.-H. Pan, Y.-M. Xu, R. Jin, D. Mandrus, X. Dai, Z. Fang, Z. Wang, and H. Ding, *Phys. Rev. Lett.* **103**, 097001 (2009).

<sup>5</sup>S. Nakatsuji, D. Hall, L. Balicas, Z. Fisk, K. Sugahara, M. Yoshioka, and Y. Maeno, *Phys. Rev. Lett.* **90**, 137202 (2003).

<sup>6</sup>A. Tamai, M. P. Allan, J. F. Mercure, W. Meevasana, R. Dunkel, D. H. Lu, R. S. Perry, A. P. Mackenzie, D. J. Singh, Z.-X. Shen, and F. Baumberger, *Phys. Rev. Lett.* **101**, 026407 (2008).

<sup>7</sup>R. A. Borzi, S. A. Grigera, R. S. Perry, N. Kikugawa, K. Kitagawa, Y. Maeno, and A. P. Mackenzie, *Phys. Rev. Lett.* **92**, 216403 (2004).

<sup>8</sup>J. Lee, M. P. Allan, M. A. Wang, J. Farrel, S. A. Grigera, F. Baumberger, J. C. Davis, and A. P. Mackenzie, *Nature Phys.* **5**, 800 (2009).

- <sup>9</sup>X. N. Lin, Z. X. Zhou, V. Durairaj, P. Schlottmann, and G. Cao, *Phys. Rev. Lett.* **95**, 017203 (2005).
- <sup>10</sup>R. S. Perry, L. M. Galvin, S. A. Grigera, L. Capogna, A. J. Schofield, A. P. Mackenzie, M. Chiao, S. R. Julian, S. Ikeda, S. Nakatsuji, Y. Maeno, and C. Pfleiderer, *Phys. Rev. Lett.* **86**, 2661 (2001).
- <sup>11</sup>R. A. Borzi, S. A. Grigera, J. Farrell, R. S. Perry, S. J. S. Lister, S. L. Lee, D. A. Tennant, Y. Maeno, and A. P. Mackenzie, *Science* **315**, 214 (2007).
- <sup>12</sup>S. Grigera, R. S. Perry, A. J. Schofield, M. Chiao, S. R. Julian, G. G. Lonzarich, S. I. Ikeda, Y. Maeno, A. J. Millis, and A. P. Mackenzie, *Science* **294**, 329 (2001).
- <sup>13</sup>G. Cao, L. Balicas, W. H. Song, Y. P. Sun, Y. Xin, V. A. Bondarenko, J. W. Brill, S. Parkin, and X. N. Lin, *Phys. Rev. B* **68**, 174409 (2003).
- <sup>14</sup>Z. Q. Mao, M. Zhou, J. Hooper, V. Golub, and C. J. O'Connor, *Phys. Rev. Lett.* **96**, 077205 (2006).
- <sup>15</sup>R. Gupta, M. Kim, H. Barath, S. L. Cooper, and G. Cao, *Phys. Rev. Lett.* **96**, 067004 (2006).
- <sup>16</sup>For  $\Delta \ll J$ , limit values of the orbital polarization are  $p = 1$  ( $n_{xy} = 2$  and  $n_{xz} + n_{yz} = 2$ , as for the  $xy$ -orbital order) and  $p = -1/2$  ( $n_{xy} = 1$  and  $n_{xz} + n_{yz} = 3$ , as in the case of the orbital-selective Mott transition).
- <sup>17</sup>V. Anisimov, I. A. Nekrasov, D. E. Kondakov, T. M. Rice, and M. Sigrist, *Eur. Phys. J. B* **25**, 191 (2002).
- <sup>18</sup>L. de Medici, S. R. Hassan, M. Capone, and X. Dai, *Phys. Rev. Lett.* **102**, 126401 (2009).
- <sup>19</sup>D. J. Singh and I. I. Mazin, *Phys. Rev. B* **63**, 165101 (2001).
- <sup>20</sup>H.-J. Noh *et al.*, *Phys. Rev. B* **72**, 052411 (2005).
- <sup>21</sup>S. J. Moon *et al.*, *Phys. Rev. B* **74**, 113104 (2006).
- <sup>22</sup>Z. Q. Mao, H. Fukazawa, and Y. Maeno, *Mater. Res. Bull.* **35**, 1813 (2000); R. Fittipaldi, A. Vecchione, S. Fusanobori, K. Takizawa, H. Yaguchi, J. Hooper, R. S. Perry, and Y. Maeno, *J. Cryst. Growth* **271**, 152 (2004); R. Fittipaldi, D. Sisti, A. Vecchione, and S. Pace, *Cryst. Growth Design* **7**, 2495 (2007).
- <sup>23</sup>R. Perry and Y. Maeno, *J. Cryst. Growth* **271**, 134 (2004).
- <sup>24</sup>M. Zhou, J. Hooper, D. Fobes, Z. Q. Mao, V. Golub, and C. J. O'Connor, *Mater. Res. Bull.* **40**, 942 (2005).
- <sup>25</sup>M. Zangrando, M. Finazzi, G. Paolucci, G. Comelli, B. Diviacco, R. P. Walker, D. Cocco, and F. Parmigiani, *Rev. Sci. Instrum.* **72**, 1313 (2001); M. Zangrando, M. Zacchigna, M. Finazzi, D. Cocco, R. Rochow, and F. Parmigiani, *ibid.* **75**, 31 (2004).
- <sup>26</sup>The total-electron-yield O  $K$ -edge spectra measured in vertical polarization at different incidence angles (i.e., different penetration depths, varying in the range 2–10 nm) show basically no angular dependence. This indicates that the electronic structure at 2–3 nm already resembles that of the bulk and is the same as that probed in the fluorescence-yield mode. Reference 31 shows that for  $\text{Sr}_2\text{RuO}_4$  the O  $K$ -edge total-electron-yield and fluorescence-yield spectra are indeed remarkably similar (including relative peak heights within one orientation) and the principal difference is the background. We obtained similar results in the cases we tested.
- <sup>27</sup>D. J. Singh, *Phys. Rev. B* **52**, 1358 (1995); T. Oguchi, *ibid.* **51**, 1385 (1995); E. Pavarini and I. I. Mazin, *ibid.* **74**, 035115 (2006).
- <sup>28</sup>E. Pavarini, S. Biermann, A. Poteryaev, A. I. Lichtenstein, A. Georges, and O. K. Andersen, *Phys. Rev. Lett.* **92**, 176403 (2004); E. Pavarini, A. Yamasaki, J. Nuss, and O. K. Andersen, *New J. Phys.* **7**, 188 (2005).
- <sup>29</sup>V. I. Anisimov, A. I. Poteryaev, M. A. Korotin, A. O. Anokhin, and G. Kotliar, *J. Phys. Condens. Matter* **9**, 7359 (1997); A. I. Lichtenstein and M. I. Katsnelson, *Phys. Rev. B* **57**, 6884 (1998).
- <sup>30</sup>A. N. Rubtsov, V. V. Savkin, and A. I. Lichtenstein, *Phys. Rev. B* **72**, 035122 (2005).
- <sup>31</sup>M. Schmidt, T. R. Cummins, M. Burk, D. H. Lu, N. Nucker, S. Schuppler, and F. Lichtenberg, *Phys. Rev. B* **53**, R14761 (1996).
- <sup>32</sup>The estimate is obtained by averaging the (horizontal) polarization and neglecting the radial part of the dipole element of the matrix.
- <sup>33</sup>Somewhat larger energy shifts (but identical trends) are obtained if the O  $2s$  electrons are treated as valence states.
- <sup>34</sup>B. Binz and M. Sigrist, *Europhys. Lett.* **65**, 816 (2004); S. Raghu, A. Paramakanti, E.-A. Kim, R. A. Borzi, S. A. Grigera, A. P. Mackenzie, and S. A. Kivelson, *Phys. Rev. B* **79**, 214402 (2009); W.-C. Lee and C. Wu, *ibid.* **80**, 104438 (2009).
- <sup>35</sup>E. Pavarini, E. Koch, and A. I. Lichtenstein, *Phys. Rev. Lett.* **101**, 266405 (2008); E. Pavarini and E. Koch, *ibid.* **104**, 086402 (2010).
- <sup>36</sup>Z. V. Pchelkina, I. A. Nekrasov, Th. Pruschke, A. Sekiyama, S. Suga, V. I. Anisimov, and D. Vollhardt, *Phys. Rev. B* **75**, 035122 (2007).
- <sup>37</sup>All states but Ru  $d$  are downfolded. For  $n = 2, 3$ , due to the  $e_g$ - $t_{2g}$  mixing, the splittings are slightly smaller if all states but the  $e_g$  are downfolded.